ACS APPLIED MATERIALS & INTERFACES

Research Article

www.acsami.org

Improving the Durability of a Drag-Reducing Nanocoating by Enhancing Its Mechanical Stability

Mengjiao Cheng,[†,‡] Songsong Zhang,[†,§] Hongyu Dong,[‡] Shihui Han,[§] Hao Wei,[§] and Feng Shi*[,‡]

[‡]State Key Laboratory of Chemical Resource Engineering & Key Laboratory of Carbon Fiber and Functional Polymer, Ministry of Education, Beijing University of Chemical Technology, Beijing 100029, China

[§]Key Laboratory of Superlight Materials and Surface Technology of Ministry of Education, Harbin Engineering University, Harbin 150001, P.R. China

Supporting Information

ABSTRACT: The durability of superhydrophobic surface is a major problem to restrict industrial application of superhydrophobic materials from laboratory research, which can be attributed to a more general issue of mechanical stability for superhydrophobic coatings. Therefore, in order to handle this issue, we have fabricated a mechanically stable drag-reducing coating composed of elastic polydimethylsiloxane (PDMS) and hydrophobic copper particles on model ships, which can resist mechanical abrasion and has displayed a durable drag-reducing effect. In comparison with normal Au superhydrophobic coatings, the as-prepared PDMS/copper coatings showed durable drag reduction performance with a similar drag-reducing rate before (26%) and after (24%) mechanical abrasion. The mechanism for the enhanced mechanical stability and maintained drag reduction of the superhydrophobic surfaces was investigated through characterizations of surface morphology, surface wettability, and water adhesive force evaluation before and after abrasion. This is the first demonstration to realize the application of durable drag reduction by improving the mechanical stability of superhydrophobic coatings. We do believe that superhydrophobic surfaces with good resistance to mechanical abrasion or scratching may draw wide attention and gain significant applications with durable drag-reducing properties.

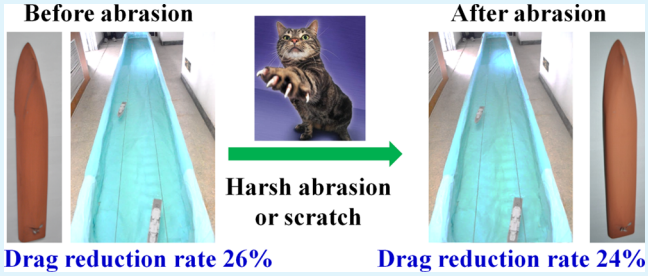

KEYWORDS: *superhydrophobic materials, durable drag reduction, mechanical stability, water adhesive force*

INTRODUCTION

Superhydrophobic surfaces have developed as a significant and attractive research topic in the field of nanoscience and nanotechnology since the first reports in 1997 by Barthlott and Neinhuis.[1,2] Until now, many reports have proposed various potential applications of superhydrophobic surfaces such as self-cleaning coatings,[3−6] antireflective films,[7,8] water/oil separation,[9−12] drag reduction,[13−15] etc. Among them, the drag-reducing property is regarded as one of the most promising and meaningful applications for practical uses.[13−17] For example, shark-skin swimsuits involved the design of superhydrophobic coatings, and have demonstrated an effective drag-reducing performance for swimming athletes to win medals.[16,17] Additionally, the drag reduction of vehicles on or under the surface of the water will save fuel consumption when sailing. However, the durability of the drag-reducing property created using superhydrophobic coatings still confronts a big challenge, just as the shark-skin swimsuit, which could only maintain its drag-reducing effect for at most 6 times. In our previous work, we achieved remarkable drag reduction rates (which was defined as $((V_{\text{superhydrophobic}} - V_{\text{normal}})/V_{\text{normal}})\cdot 100\%$) with superhydrophobic coatings on both microscale gold thread and macroscopic model ships as high as 70[13] and 49%,[14] respectively. However, the problem also existed that the drag reduction rate would drop with the number of times it was used (10 times) and even caused drag increase with longer usage. This poor durability of superhydrophobic coatings seriously restricted their further applications, especially in drag reduction. In fact, the problem of durability for drag-reducing coatings could be attributed to a more general issue of mechanical stability for superhydrophobic coatings.

In most cases, superhydrophobic coatings were obtained with two dominant factors: a suitable surface roughness combined with microscale and nanoscale structures, and a low-surface-energy coating that was normally postmodified onto the rough structures.[18−20] Therefore, mechanical abrasion will damage rough structures or remove some low-surface-energy species, which might reduce or even lose superhydrophobicity. Currently, there are two major strategies that have been proposed to address these problems. One strategy is to introduce soft and elastic materials in the construction of rough structures as they could resist external impacts by dissipating the energy with their elastic deformation.[4,21] In this respect, Vollmer's group has fabricated mechanically stable super-

Received: December 9, 2014
Accepted: February 3, 2015
Published: February 3, 2015

DOI: 10.1021/am5085012
ACS Appl. Mater. Interfaces 2015, 7, 4275−4282

hydrophobic coatings by taking advantage of fluorinated hollow silicon particles to construct rough structures that are connected by covalent bonds.[21] The other solution is to use self-healing materials for the recovery of low-surface-energy species according to the principle of minimization of surface energy. Sun et al. used this strategy to repair the damaged superhydrophobic coating through releasing healing agents of fluoroalkylsilane which was preserved within the superhydrophobic coatings.[22] Although both of the above methods were effective in increasing the mechanical stability of superhydrophobic coatings in the laboratory, there still remains a challenge to clarify whether the enhanced mechanical stability of superhydrophobic surfaces could be maintained for practical applications, such as drag-reducing nanocoatings on model ships. Therefore, we have fabricated a mechanically stable superhydrophobic coating on model ships by incorporating elastic materials (polydimethylsiloxane, PDMS) and hydrophobic copper particles, which presented enhanced durability in the drag-reducing effect. The durability of the drag reduction of the as-prepared PDMS/copper coatings was proven by checking the drag-reducing effects before and after abrasion of the model ship surfaces modified with the superhydrophobic coating. The results showed that in the presence of elastic PDMS in the as-prepared superhydrophobic coatings, the drag-reducing property was protected from abrasion while normal superhydrophobic surfaces almost lost drag reduction under similar conditions.

EXPERIMENTAL SECTION

Materials and Instruments. The following chemicals of analytical degree or materials were used as supplied: $HAuCl_4$, *n*-dodecanethiol, copper powder (200 mesh or about 74 μm, copper purity above 99%) from Sinopharm Chemical Reagent Beijing Co., Ltd., Beijing, China; copper foil tape (thickness: about 50 μm) from Shenzhen Lianli Adhesive Tape Produce Factory Co., Ltd., Shenzhen, China; note that the as-purchased copper powder was hydrophobic, as demonstrated in Figures S1 and S2 in Part 1 of Supporting Information; note that we used the copper foil tape and copper powders as supplied without any treatment; PDMS (Sylgard 184) prepolymer and its curing agent from Dow Corning, Midland, Michigan, USA; and model ships (with a feature size of 32.5 cm × 5.5 cm × 4.5 cm) equipped with an engine powered by a dry battery (1.5 V) from ZT Model Co., Ltd., Hangzhou, China. The detailed optical graph was displayed in Figure S3 in the Supporting Information, together with corresponding descriptions.

Optical photographs were taken from a Nikon camera (D5000). The contact angle and roll-off angle were measured with an OCA15EC instrument and measurements of adhesive force were carried out using a dynamic contact angle measuring device and a tensionmeter (DCAT11). Both the OCA15EC and DCAT11 instruments were from Data Physics Instruments GmbH, Filderstadt, Germany. The volume of the water droplets was 5.0 μL. Note that the data of the contact angle, roll-off angle, adhesive force and moving velocity of the model ships were obtained after repeating the experiment at least 5 to 10 times, which gave averaged results, as displayed in the figures. Scanning electron microscope (SEM) images were obtained on a Supra 55VP Field Emission Scanning Electron Microscope at 20.0 kV (Zeiss, Germany). The abrasion of all model ship surfaces was carried out by repeatedly abrading in one direction at a constant force value of about 200 mN with a contacting area about 2 cm^2 (pressure around 1.0 kPa) at an abrasion speed of 75 mm/s. For one local area, the above abrasion was carried out for at least 20 cycles. Afterward, the average weight loss percentage of the superhydrophobic model ship after abrasion was 11 ± 2%.

Fabrication of Gold (Au) Superhydrophobic Coatings on Model Ships. The model ship was cleaned with ethanol; the bottom and side surfaces that were exposed to water were totally wrapped within copper foil through pressing the adhesive copper foil tape with an average pressure of at least 9.0 ± 2.5 kPa onto the model ship surfaces (otherwise lower pressure might decrease the adhesive force between the copper foil tape and the model ship surfaces, which might lead to peeling off of the copper foil tape); then the model ship was immersed in an aqueous solution of $HAuCl_4$ (2 mg mL^{-1}) for 30 min for the formation of the rough gold aggregates, as reported in our previous work.[14] Afterward, the model ship was modified with a low-surface-energy coating of *n*-dodecanethiol by exposing the ship in a closed container with 1 mL of *n*-dodecanethiol in an oven at 30 °C for 12 h.

Fabrication of PDMS/Copper Superhydrophobic Coatings on Model Ships. The PDMS prepolymer was mixed with its curing agent at a weight ratio of 10:1 by stirring for 15 min, followed by removing bubbles with a vacuum of 50−70 Pa for 30 min. After cleaning with ethanol, the dried model ship was painted with a layer of viscous PDMS mixture (9 ± 1 mg/cm^2), after which the model ship was placed in air for 1 h for self-leveling. The flowable PDMS fluid resulted in a homogeneous surface coating in this period. Then the PDMS coating was precross-linked by heating at 60 °C for 20 min to partly cross-link the PDMS coating for the rigidity of the coating and meanwhile the surface kept sticky for further adhering of copper particles. Then the hydrophobic copper particles were continuously spread onto the partially cross-linked sticky PDMS surface until the loaded weight of copper particles reached 2.6 ± 0.2 g. Finally, the copper particles were immobilized by further fully cross-linking of PDMS; the particles that were not immobilized were washed by deionized water.

Drag Reduction Tests of Model Ships with and without Superhydrophobic Coatings. The drag reduction test was carried out in a water trough (6 m × 0.6 m × 0.3 m), as shown in Figure S4a in the Supporting Information. The water line was about 0.22-m high, leading to a water volume of 0.8 m^3 in the trough. Considering possible collision and deviation from the voyage, we have hung two parallel iron wires above water surface to act as guiding rails to adjust moving direction of the model ships. Two tiny rings with a diameter about 1 mm were adhered on two ends of the deck, which was used to connect the model ships to the iron wires through nylon thread, as illustrated in Figure S4b in the Supporting Information. For each kind of model ship, a 1.5 V battery was used as the power system and a 1-Ω resistance was cascaded. The weight of each kind of model ship was adjusted to a similar value of about 120 g. The drag reduction performance was evaluated as follows: to avoid possible delay when switching on the motor, we first turned on the motor of the model ship at the starting line and then released it. The time for each kind of model ship to complete the 6 m voyage was recorded. Then the average moving velocity (V) was calculated provided with the above voyage and time. By comparing the moving velocities of the model ships with ($V_{superhydrophobic}$) and without (V_{normal}) superhydrophobic coatings, we have defined the drag reduction rate as $((V_{superhydrophobic} - V_{normal})/V_{normal})\cdot 100\%$.

Water Adhesive Force Measurements. The water adhesive forces of the as-prepared superhydrophobic surfaces were measured with DCAT 11, which was displayed in Figure S5a in the Supporting Information. The instrument consisted of a sensitive balance to sense the force changes on the hung 5 μL water droplet and a precise motor to control the contacting-detaching process between the water droplet and the substrates. The measuring process was illustrated in Figure S5c−f in the Supporting Information. To begin with, a water droplet was hung on a holder that was connected to the upper balance detector and the superhydrophobic substrate was placed on the bottom motor. Then the test was started: the substrate was driven upward to contact the water droplet; upon contacting the detector sensed the force changes on the hung water droplet and began to collect data on the change in the force values versus the position of the motor; the substrate was set to move upward for another 0.1 mm after touching the water droplet to ensure full contact between the water droplet and the substrate; after this upward 0.1 mm movement, the substrate was taken back downward to its original position, during which the substrate was detached from the water droplet; at the moment they were totally detached, a maximum force value was

DOI: 10.1021/am5085012
ACS Appl. Mater. Interfaces 2015, 7, 4275−4282

reached, indicating the adhesive force between the water and the substrate; finally, the test finished when the substrate was back in its initial position.

RESULTS AND DISCUSSION

In our previous work, we have demonstrated remarkable drag-reducing effects of superhydrophobic coatings composed of rough gold aggregates and a low-surface-energy thiol layer on model ships.[14] The superhydrophobic coating on a large area was fabricated as follows: the cleaned model ships were wrapped thoroughly with copper foil, deposited in an aqueous solution of chloroauric acid tetrahydrate to obtain rough gold aggregates, and further modified with a low-surface-energy coating of n-dodecanethiol. The as-prepared Au superhydrophobic coating displayed a dark wine-red color, as shown in Figure 1a (left); the drag-reducing effect of the Au superhydrophobic surface was evaluated by a competitive sailing experiment with a normal model ship without any treatment in a 6 m long water trough (Figure 1b). The average moving velocities of both model ships were calculated by the time to complete the entire voyage, which were 0.31 ± 0.01 and 0.41 ± 0.01 m/s (Figure 1c), respectively; therefore, the drag reduction rate of the Au superhydrophobic surface was calculated to be around 32% (Figure 1c), which was comparable with our prior result under similar conditions.[14] However, we found that with the increasing number of sailing experiments, the drag reduction rate gradually decreased, the recession of which was especially remarkable after sailing for more than 10 times; for longer usage, the superhydrophobic coating even resulted in a drag-increasing effect. To interpret these phenomena, we hypothesized that the decline in the drag-reducing effect might be related to the mechanical stability of the as-prepared superhydrophobic coatings. To test this hypothesis, we have mechanically abraded all of the Au superhydrophobic surfaces as described in the Experimental Section, leading to an average weight loss percentage of the superhydrophobic model ship of 11 ± 2%; after the abrasion, the deposited gold aggregates easily peeled off and the coating changed to a thin and smooth surface with slight metallic luster as shown in Figure 1a (right); the film thickness change was further characterized by SEM sectional images in Figure S6 in the Supporting Information. Meanwhile, the moving velocity of the Au model ship after abrasion (0.32 ± 0.01 m/s) was quite similar to that of the normal model ship under similar conditions, and the drag-reducing rate dropped dramatically to almost 3% (Figure 1c). This result suggested that the introduced mechanical abrasion could directly lead to a decrease in the drag-reducing property.

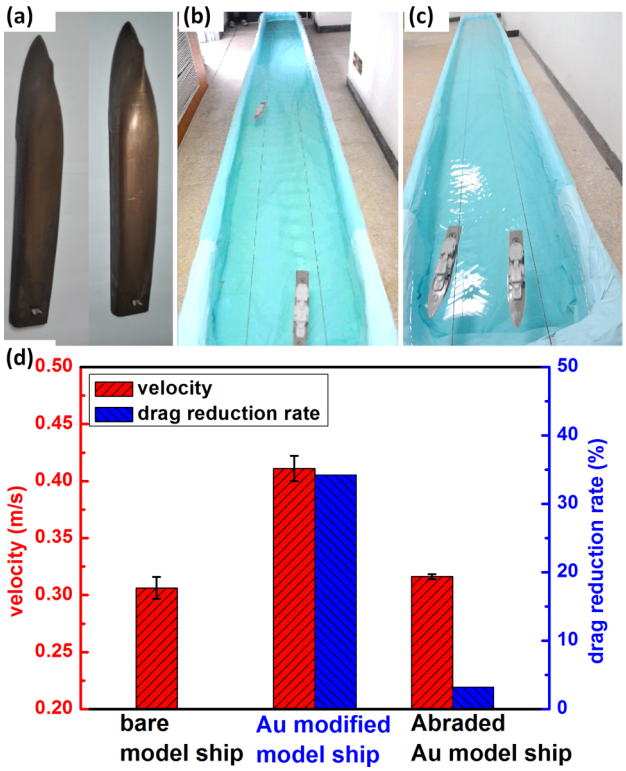

Figure 1. (a) Optical photograph of model ships modified with Au superhydrophobic coatings (left) before and (right) after mechanical abrasion. Snapshots of sailing experiments: (b) the model ship modified with Au superhydrophobic coatings before abrasion (right) reached the finishing line ahead of the normal model ship (left); (c) the Au superhydrophobic model ship after abrasion (right) completed the voyage a little faster than the normal model ship (left). (d) Left red *y* axis: moving velocity of different model ships (from left to right: normal model ship, model ship modified with Au superhydrophobic coatings before abrasion and after abrasion); right blue axis: the drag reduction rate of the Au superhydrophobic model ships before and after abrasion.

To investigate the reason for the decreased drag reduction performance after abrasion, we have characterized the surface morphology and surface wettability of the Au superhydrophobic coatings before and after mechanical abrasion, respectively. From SEM images, we could observe that before abrasion the Au superhydrophobic surface presented concave and protruding hierarchical structures of randomly distributed microscale aggregates (Figure 2a) with irregular nanostructures (Figure 2b), which contributed to sufficient surface roughness for superhydrophobicity. After surface modification with n-dodecanethiol, the surface exhibited a high contact angle of 156 ± 1 degrees and a low roll-off angle of 4 ± 1 degrees (insets of Figure 2a, b), which confirmed good superhydrophobicity of the surface. After similar abrasion of the substrates as the superhydrophobic model ship received, the surface morphology changed remarkably: the majority of protruding aggregates disappeared and left large areas of smooth zones, as shown in Figure 2c; from the local magnification in Figure 2d, we found that only a few particles remained on the flat surface and the surface roughness decreased compared with the roughness before the harsh mechanical damage. Correspondingly, the contact angle of the abraded surface decrease to 117 ± 5°, as shown in the inset of Figure 2c, which was far below 150° and should be regarded as hydrophobicity instead of superhydrophobicity. Additionally, the surface exhibited a strong adhesion to water so that the water droplets did not roll off even at 90° (inset of Figure 2d). The decreased superhydrophobicity and increased water adhesion should be attributed to the following two factors: the damage of rough structures confirmed by the change of surface morphology before and after abrasion, and the loss of the low-surface-energy coating in the abrasion process because of bare gold and/or copper foil with a high surface energy being exposed once the original outmost rough gold coated with n-dodecanethiol had peeled off. The above phenomena demonstrated that the Au superhydrophobic coating showed poor mechanical stability of superhydrophobicity toward external abrasion. There are reports considering that decreased

DOI: 10.1021/am5085012
ACS Appl. Mater. Interfaces 2015, 7, 4275−4282

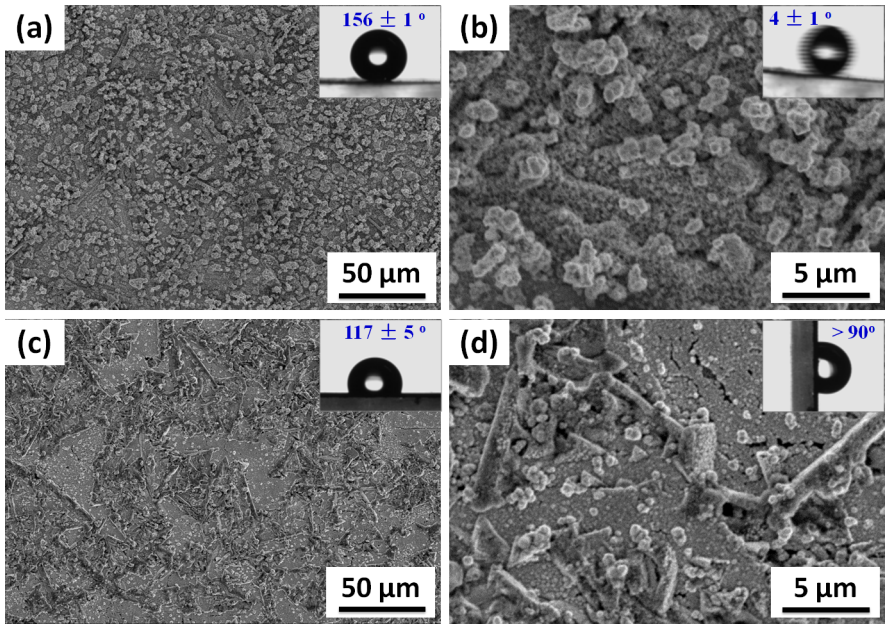

Figure 2. SEM images of Au superhydrophobic surfaces (a) before abrasion and (b) its local magnification, (c) after abrasion and (d) its corresponding magnified image. The insets of a and c correspond to the contact angle of the surface; the insets of b and d are roll-off angles before and after abrasion of the Au superhydrophobic surfaces, respectively.

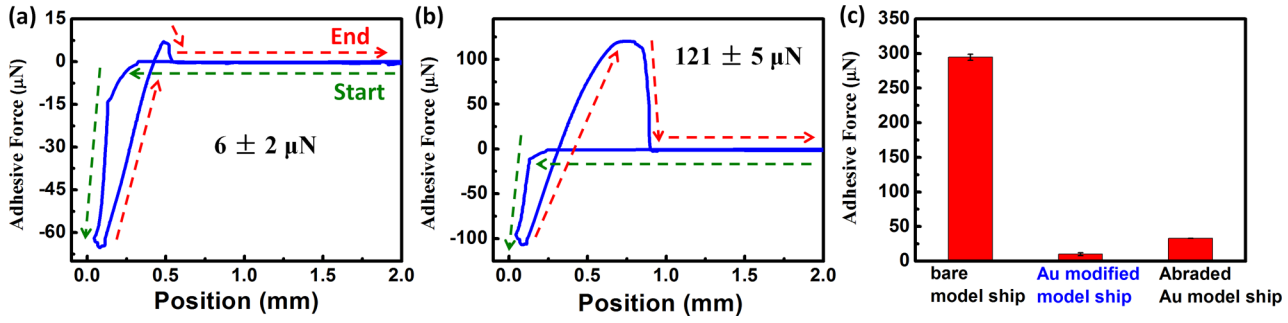

Figure 3. Water adhesive force curves of the Au superhydrophobic coatings (a) before and (b) after abrasion. (c) The force values of the bare model ship, and model ships with Au superhydrophobic coatings before and after abrasion.

superhydrophobicity and high contact angle hysteresis led to poor drag reduction performance,[23−25] which corresponds with the above experimental sailing results.

Whether the destroyed surface morphology and changed wetting property after mechanical abrasion would lead to a decline in the drag reduction rate in theory was further confirmed by measurement of water adhesive force, which acted as a criteria for determining drag reduction performance.[15] The water adhesive force curve was obtained by recording force changes in the contacting−separating process between tested substrates and a water droplet, as described in the Experimental Section in detail and illustrated in Figure S5 in the Supporting Information. For typical force curves (Figure 3a, b), before the substrate rose to touch the hanging water droplet, the force values were near zero because the balance detector at the top connected to the water droplet did not sense any force changes on the water droplet. When the substrate made contact with the water droplet, the substrate provided an extra supporting force for the water droplet and meanwhile the water droplet was repelled by the substrate, leading to a drop in the force values to a negative level. After the substrate was set to move toward the water droplet for 0.1 mm after first contact, the substrate moved back to its original position, during which the substrate and the water droplet separated; because of the detachment, the supporting force from the substrate gradually disappeared and simultaneously water adhesion toward the substrate produced a downward dragging force, contributing to the increased force value to positive values. At the total detaching point between the substrate and the water droplet, the maximum force value was obtained, which indicated the adhesive force of the substrate toward water. After total separation, the final force level could still be near zero if the substrate captured no water or dropped to negative values if the water was captured by the substrate from the droplet, which would have led to drag reduction or increase, respectively.

For comparison, the surface wettability and water adhesion property of the normal model ship without any surface modification were taken as a control. The bare model ship surface, made of plastic, was near hydrophobic with a contact angle of 85 ± 2 degrees and the water adhesion was serious because the roll-off angle exceeded 90 deg. Because of the high water adhesion, the measured water adhesive force value was as high as 295 ± 4 μN, which we could observe from the force curve (Figure S8 in the Supporting Information). The force curve indicated that water partly remained on the surface after

DOI: 10.1021/am5085012
ACS Appl. Mater. Interfaces 2015, 7, 4275−4282

detachment of the water droplet and the surface in the measurement, which could be understood by the hydrophilic nature of the surface. For the as-prepared Au superhydrophobic coating, the water adhesive force was as small as 6 ± 2 μN, which was only 2% of the value of the blank model ship. Additionally, the status of the force curve showed that no water was captured (Figure 3a) and suggested a drag-reducing property according to the metric for determining the drag reduction of superhydrophobic coatings.[15] Since there was no water captured after total separation for the Au superhydrophobic coating before abrasion and the adhesive force value was low, the prediction of drag reduction performance matched well with the above drag reduction result of 32%. However, after a large area of mechanical abrasion throughout the model ship surfaces, the water adhesive force value dramatically increased to 121 ± 5 μN, which was almost 22 times of that before abrasion. Because the curve of water adhesive force under this condition still showed no water captured on the substrate (Figure 3b), this coating still achieved a drag-reducing property with a low rate of 3%. The remarkable fall in the drag reduction rate could be predicted by the remarkable increase in water adhesive force from 6 ± 2 to 121 ± 5 μN. Both the results of water capture status and water adhesive force values fit well with the drag reduction performance before and after abrasion.

To address the poor durability in drag reduction through superhydrophobic coatings, we have introduced an elastic material, PDMS, to enhance the mechanical stability of superhydrophobic coatings by integrating PDMS and hydrophobic copper particles to the coating:[15] the model ships were cleaned with ethanol and painted with a layer of PDMS mixture of its prepolymer and curing agent, followed by keeping it in the air for 1 h to allow for self-flowing of the viscous PDMS mixture to form a homogeneous surface coating. The PDMS coating was then pre-cross-linked by heating for 20 min to obtain a partially cross-linked film with stickiness and a better strength compared with the viscous PDMS fluid. Thus, this sticky surface could adhere to the commercially available hydrophobic copper particles with a surface energy of 26.7 mN/m;[15] because of the stiffness partially resulting from the cross-linked PDMS coating, the copper particles would be partly wrapped by the PDMS layer and further immobilized through a total cross-linking of PDMS, whose covalent cross-linking density was (9.0 ± 0.1) × 10^{-5} mol/cm^3 (Part 7 in the Supporting Information). The as-prepared PDMS/copper superhydrophobic coating on the model ship presented a dark rose-bengal color, as shown in Figure 4a (left).

After we obtained the PDMS/copper superhydrophobic coating on model ships, we wondered whether it exhibited a durable drag reduction effect. Similar sailing experiments to the as-prepared superhydrophobic coating were carried out in the same water trough (Figure 4b). The model ship with the PDMS/copper coating showed an average moving velocity of about 0.39 ± 0.01 m/s, which was a bit lower than the Au superhydrophobic model ship (0.41 ± 0.01 m/s) but much larger than the normal one (0.31 ± 0.01 m/s). The reason for the lower velocity of PDMS/copper modified model ship compared with the Au-modified model ship was the poorer superhydrophobicity and higher water adhesive force of the PDMS/copper superhydrophobic coating, as discussed later. Compared with the control model ship, the PDMS/copper modified ship exhibited a drag reduction rate of 26% (Figure 4c). The contribution of PDMS and hydrophobic copper

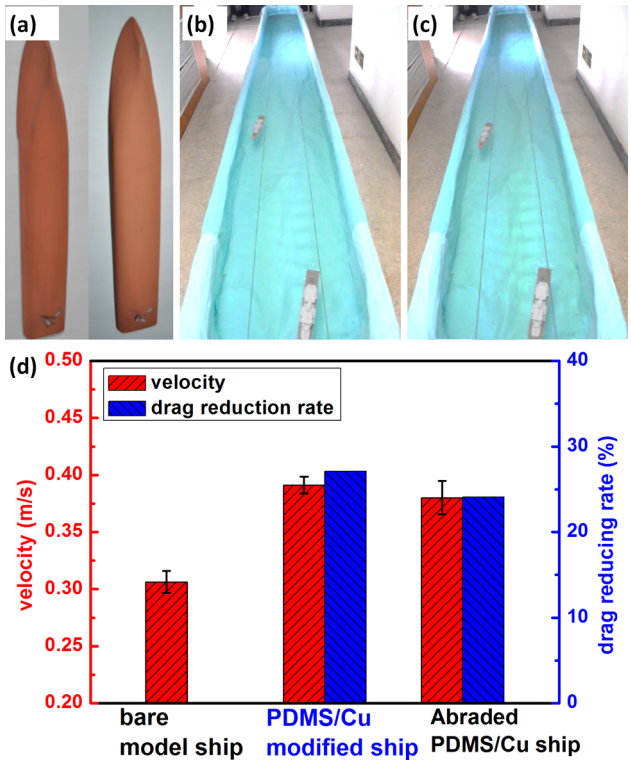

Figure 4. (a) Optical photograph of model ships modified with PDMS/copper superhydrophobic coatings (left) before and (right) after mechanical abrasion. Snapshots of sailing experiments: (b) the model ship modified with PDMS/copper superhydrophobic coatings before abrasion (right) reached the finishing line ahead of the normal model ship (left); (c) the PDMS/copper superhydrophobic model ship after abrasion (right) completed the voyage much faster than the normal model ship (left). (d) Left red *y* axis: moving velocity of different model ships (from left to right: normal model ship, model ship modified with PDMS/copper superhydrophobic coatings before abrasion and after abrasion); right blue axis: corresponding to the drag reduction rate of the PDMS/copper superhydrophobic model ships before and after abrasion.

particles to drag reduction were discussed in Part 8 in the Supporting Information. The durability of drag reduction was further checked after similar abrasion as the treatment of Au superhydrophobic coating, leading to an average weight loss percentage of the superhydrophobic model ship of 11 ± 2%. The appearance of the PDMS/copper coating on the model ship turned from a dark to a light rose-bengal color (Figure 4a, right) after entire abrasion of the model ship surfaces, but the majority of the coating remained because of the presence of the cross-linked PDMS layer. The film thickness change was demonstrated in Figure S7 in the Supporting Information. The change in color might be caused by the peeling off of loosely adhered copper particles during the abrasion, but those largely trapped within the PDMS layer kept stable due to their immobilization by covalent bonding. The drag-reducing property of the abraded PDMS/copper superhydrophobic coating was re-evaluated through a similar sailing experiment, and the obtained drag reduction rate of 24% did not change much when compared with the value of 26% before abrasion. The results were summarized in Figure 4c, which clearly show that after abrasion, the percentage decrease of the drag-reducing effect for the PDMS/copper superhydrophobic coating (6.6%) was much smaller than that of the Au

DOI: 10.1021/am5085012
ACS Appl. Mater. Interfaces 2015, 7, 4275−4282

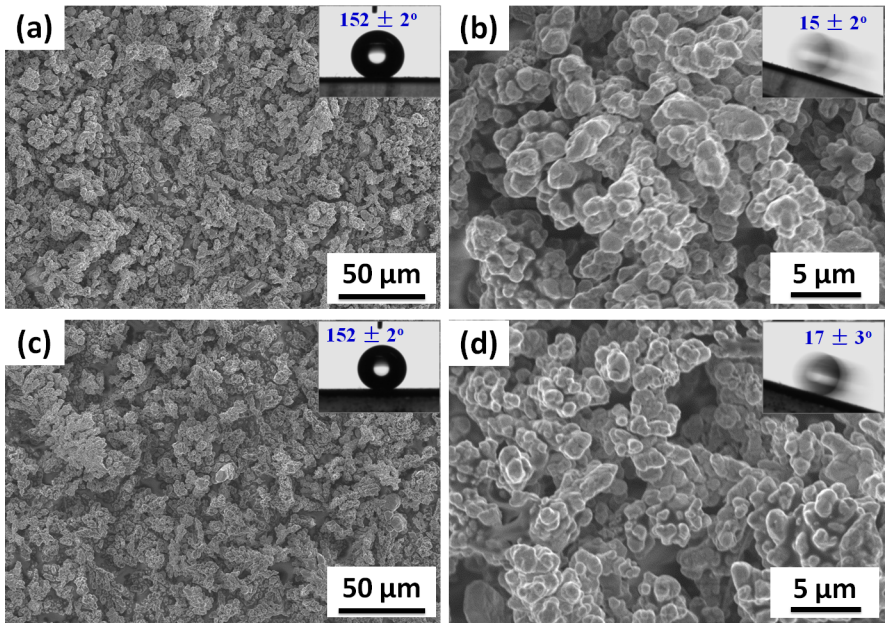

Figure 5. SEM images of PDMS/copper superhydrophobic surfaces (a) before abrasion and (b) its local magnification, (c) after abrasion and (d) its corresponding magnified image. The insets of a and c correspond to the contact angle of the surface; the insets of b and d are roll-off angles before and after abrasion of the PDMS/copper superhydrophobic surfaces, respectively.

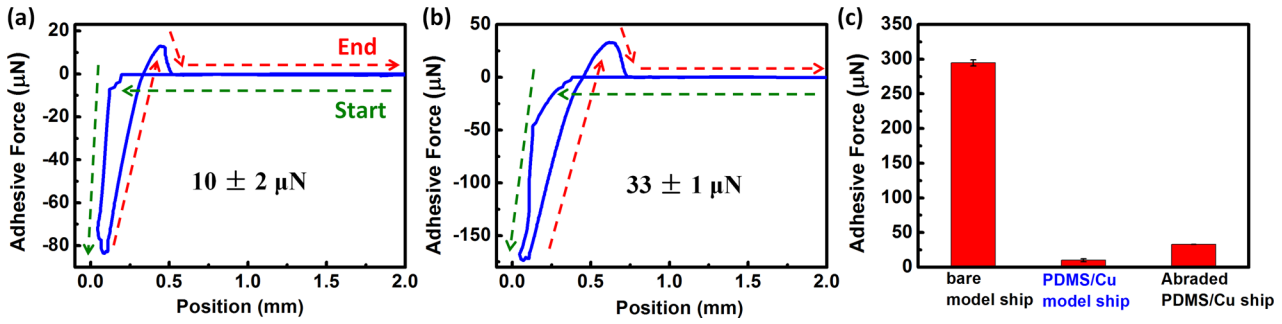

Figure 6. Water adhesive force curves of the PDMS/copper superhydrophobic coatings (a) before and (b) after abrasion. (c) The force values of the bare model ship, and model ships with PDMS/copper superhydrophobic coatings before and after abrasion.

superhydrophobic coating (90.1%). Moreover, to evaluate the effect of abraded degree on the drag reduction performance, we have correlated the weight loss percentage of model ship after abrasion with the drag reduction rate in Part 9 in the Supporting Information. The results showed that when the weight loss increased to 18%, the drag reducing performance was maintained and could reach a drag reduction rate of 16%. Therefore, the current PDMS/copper coating did show improved durability of the drag-reducing property of superhydrophobic coatings.

To check whether the durable drag reduction was realized through enhanced mechanical stability of superhydrophobic surfaces, we have compared the superhydrophobicity of the PDMS/copper coatings before and after abrasion through characterization of surface morphology and wettability. As shown in Figure 5a, the as-prepared PDMS/copper surface showed rough irregular structures with microscale as well as nanoscale aggregates, which were caused by the composites of PDMS and copper particles. The irregular aggregation of copper particles above the PDMS coating not only provided sufficient surface roughness but also achieved good film stability because of cross-linking through the covalent bond that held the particles. Additionally, no further surface modification of low-surface-energy species were needed because both the protruding copper particles and some exposed PDMS have a low surface energy, leading to a high contact angle of 152 ± 1° and a low roll-off angle of 15 ± 2° (insets of Figure 5a, b). The PDMS coating acted as the supporting layer as well as a strong connection between the rough copper structures and the model ship. Therefore, after serious mechanical abrasion of a large area, we could observe that rough hierarchical structures with three-dimensional micronano aggregates still remain from the SEM images of the abraded coating (Figure 5c, d); the surface morphology was almost similar to that before abrasion. Correspondingly, the contact angle before and after abrasion were the same value of 152 ± 2°, indicating that the superhydrophobicity was not affected by the abrasion and peeling off of the outmost copper particles. In addition, the roll-off angle changed slightly from 15 ± 2° to 17 ± 3°. The maintained superhydrophobicity and low contact angle hysteresis is favored for good drag reduction according to most reports,[23−25] and matched well with the above experimental sailing results.

Although the water adhesive forces increased a little from the original 10 ± 2 μN to 33 ± 1 μN (Figure 6), the water capture status was the same after abrasion, both of which fit well with

DOI: 10.1021/am5085012
ACS Appl. Mater. Interfaces 2015, 7, 4275−4282

the metric for determining the drag-reducing effect of superhydrophobic coatings in theory and the sailing results in practice. One thing should be mentioned that the lower contact angle, higher roll-off angle and larger water adhesive force value of the PDMS/copper coating compared with the Au coating resulted a lower moving velocity of 0.39 ± 0.01 m/s for the model ship with PDMS/copper coating than that of 0.41 ± 0.01 m/s for the ship with Au coating. The reason was that both the contact angle hysteresis and water adhesive force metric indicated a better drag reduction performance of the Au coating,[23−25] which had lower contact angle hysteresis and adhesive force values. However, the mechanical stability of the superhydrophobicity for PDMS/copper coating was highly enhanced compared with the Au superhydrophobic surface. The reason for the stable superhydrophobicity of PDMS/copper coating against abrasion was interpreted as follows: (1) the covalently cross-linked PDMS played an important role in the immobilization of rough structures, which provided strong adhesion to the model ship surfaces and the rough aggregates of the copper particles; (2) both PDMS and copper particles were hydrophobic, which contributed to the low surface energy required for superhydrophobicity; even after abrasion, the newly exposed surface still exhibited a low-surface-energy; (3) the elastic property of PDMS could have helped to resist external impact by consuming energy through deformation. These features are all favorable for the protection of superhydrophobicity from mechanical abrasion or scratching. In addition, the long-term stability,[26] thermal stability, and pressure resistant property of the PDMS/copper superhydrophobic coating are evaluated in Part 10 in the Supporting Information to support the durability of this coating. Because of the well-maintained superhydrophobicity and tiny increase in water adhesion, the drag reduction rate of the PDMS/copper superhydrophobic coating only decreased a little. Thus, we considered that the durability of the drag-reducing property of superhydrophobic coatings could be improved through enhancing the mechanical stability of superhydrophobic surfaces.

CONCLUSION

To summarize, we have obtained a mechanically stable superhydrophobic coating composed of elastic PDMS and hydrophobic copper particles on model ships, which can resist mechanical abrasion and which displayed a durable drag-reducing effect. The mechanism for the enhanced mechanical stability of superhydrophobic surfaces was investigated through a characterization of surface morphology and surface wettability before and after abrasion. The contribution from the stable superhydrophobicity to durable drag reduction was demonstrated by sailing experiments of model ships with superhydrophobic coatings before and after mechanical damage. This is the first demonstration to show the application of durable drag reduction by improving the mechanical stability of superhydrophobic coatings. We do believe that superhydrophobic surfaces with good resistance to mechanical abrasion or scratching may draw wide attention and gain significant applications with the durable drag-reducing property.

ASSOCIATED CONTENT

Supporting Information

Wettability of as-purchased copper powders; detailed description of model ship; illustration of sailing tests and water adhesive measurements; SEM sectional views of superhydrophobic coatings before and after abrasion; water adhesive force of bare model ship; covalent crosslinking density of PDMS/copper coating; contribution of PDMS and hydrophobic copper particles alone to drag reduction; effects of abraded degree on drag reduction; long-term stability, thermal stability and pressure resistant property of PDMS/copper coating. This material is available free of charge via the Internet at http://pubs.acs.org.

AUTHOR INFORMATION

Corresponding Author

*E-mail: shi@mail.buct.edu.cn.

Author Contributions

†M.C. and S.Z. contributed equally. The manuscript was written through contributions of all authors. All authors have given approval to the final version of the manuscript.

Notes

The authors declare no competing financial interest.

ACKNOWLEDGMENTS

This work was supported by NSFC (21374006; 51422302), the Program of the Co-Construction with Beijing Municipal Commission of Education of China, the Fok Ying Tung Education Foundation (131013), Open Project of State Key Laboratory of Supramolecular Structure and Materials (SKLSSM201501), and Beijing Young Talents Plan (YETP0488).

REFERENCES

(1) Barthlott, W.; Neinhuis, C. Purity of the Sacred Lotus, or Escape from Contamination in Biological Surfaces. *Planta* **1997**, *202*, 1−8.

(2) Neinhuis, C.; Barthlott, W. Characterization and Distribution of Water-repellent, Self-cleaning Plant Surfaces. *Ann. Bot.* **1997**, *79*, 667−677.

(3) Nishimoto, S.; Bhushan, B. Bioinspired Self-Cleaning Surfaces with Superhydrophobicity, Superoleophobicity, and Superhydrophilicity. *RSC Adv.* **2013**, *3*, 671−690.

(4) Deng, X.; Mammen, L.; Butt, H. J.; Vollmer, D. Candle Soot as a Template for a Transparent Robust Superamphiphobic Coating. *Science* **2012**, *335*, 67−70.

(5) Shen, L. Y.; Wang, B. L.; Wang, J. L.; Fu, J. H.; Picart, C.; Ji, J. Asymmetric Free-Standing Film with Multifunctional Anti-Bacterial and Self-Cleaning Properties. *ACS Appl. Mater. Interfaces* **2012**, *4*, 4476−4483.

(6) Xue, C.-H.; Li, Y.-R.; Zhang, P.; Ma, J.-Z.; Jia, S.-T. Washable and Wear-Resistant Superhydrophobic Surfaces with Self-Cleaning Property by Chemical Etching of Fibers and Hydrophobization. *ACS Appl. Mater. Interfaces* **2014**, *6*, 10153−10161.

(7) Zhang, L. B.; Li, Y.; Sun, J. Q.; Shen, J. C. Mechanically Stable Antireflection and Antifogging Coatings Fabricated by the Layer-by-Layer Deposition Process and Postcalcination. *Langmuir* **2008**, *24*, 10851−10857.

(8) Yildirim, A.; Khudiyev, T.; Daglar, B.; Budunoglu, H.; Okyay, A. K.; Bayindir, M. Superhydrophobic and Omnidirectional Antireflective Surfaces from Nanostructured Ormosil Colloids. *ACS Appl. Mater. Interfaces* **2013**, *5*, 853−860.

(9) Zhang, W. B.; Shi, Z.; Zhang, F.; Liu, X.; Jin, J.; Jiang, L. Superhydrophobic and Superoleophilic PVDF Membranes for Effective Separation of Water-in-Oil Emulsions with High Flux. *Adv. Mater.* **2013**, *25*, 2071−2076.

(10) Ju, G. N.; Cheng, M. J.; Shi, F. A pH-Responsive Smart Surface for the Continuous Separation of Oil/Water/Oil Ternary Mixtures. *NPG Asia Mater.* **2014**, *6*, e111.

DOI: 10.1021/am5085012
ACS Appl. Mater. Interfaces 2015, 7, 4275−4282

(11) Cheng, M. J.; Ju, G. N.; Jiang, C.; Zhang, Y. J.; Shi, F. Controlled Exponential Growth in Layer-by-layer Multilayers Using High Gravity Fields. *J. Mater. Chem. A* **2013**, *1*, 13411−14053.
(12) Liu, N.; Cao, Y. Z.; Lin, X.; Chen, Y. N.; Feng, L.; Wei, Y. A Facile Solvent-Manipulated Mesh for Reversible Oil/Water Separation. *ACS Appl. Mater. Interfaces* **2014**, *6*, 12821−12826.
(13) Shi, F.; Niu, J.; Liu, J. L.; Liu, F.; Wang, Z. Q.; Feng, X.-Q.; Zhang, X. Towards Understanding Why a Superhydrophobic Coating is Needed by Water Striders. *Adv. Mater.* **2007**, *19*, 2257−2261.
(14) Dong, H. Y.; Cheng, M. J.; Zhang, Y. J.; Wei, H.; Shi, F. Extraordinary Drag-Reducing Effect of a Superhydrophobic Coating on a Macroscopic Model Ship at High Speed. *J. Mater. Chem. A* **2013**, *1*, 5886−5891.
(15) Cheng, M. J.; Song, M. M.; Dong, H. Y.; Shi, F. Surface Adhesive Forces: A Metric Describing the Drag-Reducing Effects of Superhydrophobic Coatings. *Small* **2014**, DOI: 10.1002/smll.201402618.
(16) Ball, P. Engineering Shark skin and Other Solutions. *Nature* **1999**, *400*, 507−509.
(17) Krieger, K. Do Pool Sharks Swim Faster? *Science* **2004**, *305*, 636−637.
(18) Xia, F.; Jiang, L. Bio-Inspired, Smart, Multiscale Interfacial Materials. *Adv. Mater.* **2008**, *20*, 2842−2858.
(19) Yao, X.; Song, Y. L.; Jiang, L. Applications of Bio-Inspired Special Wettable Surfaces. *Adv. Mater.* **2011**, *23*, 719−734.
(20) Liu, X. J.; Liang, Y. M.; Zhou, F.; Liu, W. M. Extreme Wettability and Tunable Adhesion: Biomimicking beyond Nature? *Soft Matter* **2012**, *8*, 2070−2086.
(21) Deng, X.; Mammen, L.; Zhao, Y. F.; Lellig, P.; Müllen, K.; Li, C.; Butt, H.-J.; Vollmer, D. Transparent, Thermally Stable and Mechanically Robust Superhydrophobic Surfaces Made from Porous Silica Capsules. *Adv. Mater.* **2011**, *23*, 2962−2965.
(22) Li, Y.; Li, L.; Sun, J. Q. Bioinspired Self-Healing Superhydrophobic Coatings. *Angew. Chem., Int. Ed.* **2010**, *49*, 6129−6133.
(23) Vinogradova, O. I.; Dubov, A. L. Superhydrophobic Textures for Microfluidics. *Mendeleev Commun.* **2012**, *22*, 229−236.
(24) Lv, P. Y.; Xue, Y. H.; Shi, Y. P.; Lin, H.; Duan, H. L. Metastable States and Wetting Transition of Submerged Superhydrophobic Structures. *Phys. Rev. Lett.* **2014**, *112*, 196101.
(25) Xue, Y. H.; Chu, S. G.; Lv, P. Y.; Duan, H. L. Importance of Hierarchical Structures in Wetting Stability on Submersed Superhydrophobic Surfaces. *Langmuir* **2012**, *28*, 9440−9450.
(26) Ellinas, K.; Pujari, S. P.; Dragatogiannis, D. A.; Charitidis, C. A.; Tserepi, A.; Zuilhof, H.; Gogolides, E. Plasma Micro-Nanotextured, Scratch, Water and Hexadecane Resistant, Superhydrophobic, and Superamphiphobic Polymeric Surfaces with Perfluorinated Monolayers. *ACS Appl. Mater. Interfaces* **2014**, *6*, 6510−6524.

DOI: 10.1021/am5085012
ACS Appl. Mater. Interfaces 2015, 7, 4275−4282